Differential processing of *Arabidopsis* ubiquitin-like Atg8 autophagy proteins by Atg4 cysteine proteases

Jongchan Woo[a], Eunsook Park[b], and S. P. Dinesh-Kumar[a,1]

[a]Department of Plant Biology and the Genome Center, College of Biological Sciences, and [b]Department of Plant Sciences, College of Agricultural and Environmental Sciences, University of California, Davis, CA 95616

Edited* by Patricia C. Zambryski, University of California, Berkeley, CA, and approved December 6, 2013 (received for review September 27, 2013)

Autophagy is a highly conserved biological process during which double membrane bound autophagosomes carry intracellular cargo material to the vacuole or lysosome for degradation and/or recycling. Autophagosome biogenesis requires Autophagy 4 (Atg4) cysteine protease-mediated processing of ubiquitin-like Atg8 proteins. Unlike single *Atg4* and *Atg8* genes in yeast, the *Arabidopsis* genome contains two *Atg4* (*AtAtg4a* and *AtAtg4b*) and nine *Atg8* (*AtAtg8a–AtAtg8i*) genes. However, we know very little about specificity of different AtAtg4s for processing of different AtAtg8s. Here, we describe a unique bioluminescence resonance energy transfer-based AtAtg8 synthetic substrate to assess AtAtg4 activity in vitro and in vivo. In addition, we developed a unique native gel assay of superhRLUC catalytic activity assay to monitor cleavage of AtAtg8s in vitro. Our results indicate that AtAtg4a is the predominant protease and that it processes AtAtg8a, AtAtg8c, AtAtg8d, and AtAtg8i better than AtAtg4b in vitro. In addition, kinetic analyses indicate that although both AtAtg4s have similar substrate affinity, AtAtg4a is more active than AtAtg4b in vitro. Activity of AtAtg4s is reversibly inhibited in vitro by reactive oxygen species such as H_2O_2. Our in vivo bioluminescence resonance energy transfer analyses in *Arabidopsis* transgenic plants indicate that the AtAtg8 synthetic substrate is efficiently processed and this is AtAtg4 dependent. These results indicate that the synthetic AtAtg8 substrate is used efficiently in the biogenesis of autophagosomes in vivo. Transgenic *Arabidopsis* plants expressing the AtAtg8 synthetic substrate will be a valuable tool to dissect autophagy processes and the role of autophagy during different biological processes in plants.

atg4a4b | nitrogen starvation | autophagic body | monodansylcadaverine

Macroautophagy, hereafter referred to as autophagy, is an evolutionarily conserved biological process from yeast to higher eukaryotes including plants (1–4). During autophagy, intracellular components are enclosed in double membrane vesicles called autophagosomes. Cargoes in autophagosomes are then delivered to the vacuole or the lysosome for degradation or recycling. Biogenesis of autophagosomes requires conjugation of phosphatidylethanolamine (PE) to ubiquitin-like Atg8 proteins (1, 5). Before PE conjugation, the Atg8 protein is posttranslationally processed by Atg4 cysteine protease at the conserved C-terminal glycine (Gly) residue (6). The exposed Gly residue is then implicated in adduct with PE. Atg4 is also required for a deconjugation step in which Atg8-PE is removed from the outer membrane of autophagosome for Atg8 recycling and autophagosome completion (7, 8).

Compared with single *Atg4* and *Atg8* genes in yeast, the *Arabidopsis* genome contains two *AtAtg4* (*AtAtg4a* and *AtAtg4b*) and nine *AtAtg8* (*AtAtg8a–AtAtg8i*) genes (9, 10). However, we know very little about specificity of different AtAtg4s for processing of different AtAtg8 isoforms. Because *AtAtg4* and *AtAtg8* genes are differentially regulated under different environmental conditions, we and others have proposed that the expansion of *AtAtg4* and *AtAtg8* members may provide specificity for activating autophagy during different biological processes (11–13).

To test differential activity of AtAtg4s, we have systematically investigated the specificity of AtAtg4a and AtAtg4b cysteine proteases for processing of different AtAtg8s. For this, we designed unique AtAtg8 synthetic substrates and developed a sensitive method to follow the processing of AtAtg8s. Our results indicate that AtAtg4a is a predominant protease and it processes AtAtg8a, AtAtg8c, AtAtg8d, and AtAtg8i better than AtAtg4b in vitro. In addition, kinetic analyses indicate that although both AtAtg4s have similar substrate affinity, AtAtg4a is more active than AtAtg4b in vitro. The AtAtg8 synthetic substrate is also efficiently processed in vivo in *Arabidopsis* transgenic plants and this processing requires endogenous AtAtg4 proteases. Transgenic *Arabidopsis* plants expressing the AtAtg8a synthetic substrate described here will be a valuable tool to dissect the autophagy process and its role in different biological processes.

Results

Unique AtAtg8 Synthetic Substrates to Monitor Specificity of AtAtg4 Cysteine Proteases. To gain insights into AtAtg4 substrate specificity to different AtAtg8s, we designed unique AtAtg8 synthetic substrates. In these substrates, Citrine fluorescent protein (C) and modified *Renilla* luciferase superhRLUC (ShR) (14) were fused to the N- and C termini of AtAtg8, respectively (C-AtAtg8-ShR) (Fig. 1*B*). In in vitro assay, AtAtg4-mediated cleavage of AtAtg8 synthetic substrates at the conserved Gly residue in the C terminus (Fig. 1*A*) will result in the generation of C-AtAtg8 and ShR byproducts (Fig. 1*B*). The cleaved ShR byproduct can easily be separated from the full-length uncleaved AtAtg8 synthetic substrate on a native polyacrylamide gel (Fig. 1*B*). The cleaved

Significance

Autophagy is a highly regulated biological process for recycling or degrading cellular contents in response to environmental stimuli. Atg4 cysteine protease-mediated processing of Atg8 proteins is required for formation of intracellular vesicles, autophagosomes, which carry cellular cargoes to the vacuole/lysosome. Because the *Arabidopsis* plant contains nine AtAtg8 and two AtAtg4 proteins, we have developed unique AtAtg8 synthetic substrates to determine AtAtg4s cleavage specificity. We show that AtAtg4a is more active and cleaves all AtAtg8s efficiently compared with AtAtg4b. The AtAtg8 synthetic substrate can be efficiently incorporated to autophagosomes in plant cells and this requires endogenous AtAtg4s. The AtAtg8 synthetic substrates described here are suitable to screen for in vitro and in vivo autophagy regulators.

Author contributions: J.W. and S.P.D.-K. designed research; J.W. and E.P. performed research; J.W., E.P., and S.P.D.-K. analyzed data; and J.W., E.P., and S.P.D.-K. wrote the paper.

The authors declare no conflict of interest.

*This Direct Submission article had a prearranged editor.

[1]To whom correspondence should be addressed. E-mail: spdineshkumar@ucdavis.edu.

This article contains supporting information online at www.pnas.org/lookup/suppl/doi:10.1073/pnas.1318207111/-/DCSupplemental.

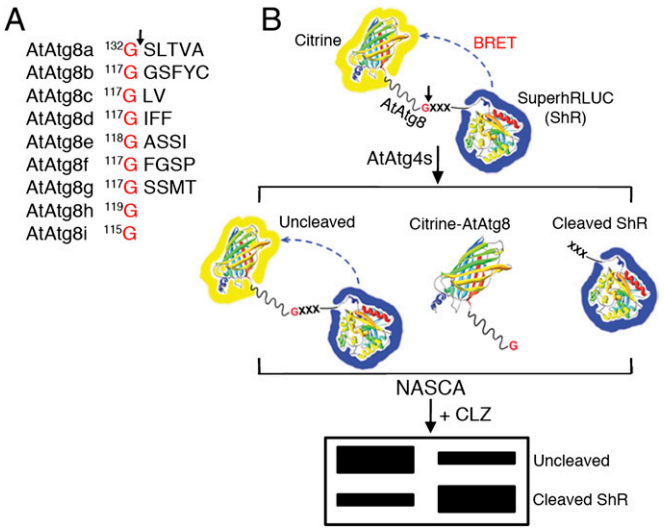

Fig. 1. Schematics of BRET-based AtAtg8 synthetic substrate and NASCA assay. (*A*) The conserved glycine (G) residue at the C terminus of AtAtg8s is shown. Arrow indicates the site of cleavage by AtAtg4 cysteine proteases. (*B*) In the BRET-based AtAtg8 substrates, Citrine and modified *Renilla* luciferase, SuperhRLUC (ShR) were fused to the amino and the carboxyl terminus of AtAtg8, respectively. Cleavage of this substrate by AtAtg4 will generate Citrine-AtAtg8 and ShR byproducts. In addition, some of the substrate may remain uncleaved. The amount of cleaved ShR byproduct can be separated from the uncleaved AtAtg8 substrate on a native polyacrylamide gel electrophoresis followed by direct detection in the presence of a luciferase substrate, coelenterazine (CLZ). XXX indicates additional amino acids after the conserved G of AtAtg8s except AtAtg8h and AtAtg8i.

ShR byproduct can then be monitored and quantified directly on the native PAGE gel in the presence of the luciferase substrate, coelenterazine (CLZ). We refer to this method as native gel assay of superhRLUC catalytic activity (NASCA). In addition, full-length uncleaved and cleaved byproducts can be monitored by separating them on SDS/PAGE followed by immunoblotting with RLUC antibodies. The AtAtg8 synthetic substrates in combination with NASCA provide a fast, easy, and versatile method to investigate substrate specificity of AtAtg4s to different AtAtg8s in vitro.

These AtAtg8 synthetic substrates could also be used to monitor AtAtg8 cleavage efficiency in plant cells using bioluminescence resonance energy transfer (BRET) assay (15) because the absorption spectrum of Citrine (λ_{max} = 516 nm) overlaps well with the emission spectrum of the ShR energy donor (λ_{max} = 475 nm) (14). We hypothesized that the uncleaved C-AtAtg8-ShR allows BRET to occur in the presence of CLZ because of the close proximity between Citrine and ShR. However, cleavage of the C-AtAtg8-ShR synthetic substrate by AtAtg4s will result in separation of Citrine and ShR and hence results in significant reduction of BRET ratio (yellow fluorescence/blue luminescence). Therefore, this method will be highly efficient for comparison between uncleaved and cleaved synthetic substrates processed by AtAtg4s under in vivo conditions.

AtAtg4a and AtAtg4b Cysteine Proteases Selectively Process Different AtAtg8 Isoforms. To assess whether AtAtg4a and AtAtg4b cysteine proteases exhibit differential specificity toward processing of different AtAtg8s, we performed NASCA assays. We expressed and purified AtAtg4a and AtAtg4b fused to maltose binding protein (MBP) and C-AtAtg8-ShR synthetic substrates fused to 6×HIS using a bacterial expression system (Fig. S1 and *SI Materials and Methods*). All nine purified Atg8s (AtAtg8a–AtAtg8i) were tested for cleavage with AtAtg4a and AtAtg4b separately. AtAtg4a cleaved AtAtg8a, AtAtg8c, AtAtg8d, and AtAtg8i more efficiently compared with AtAtg4b because more cleaved ShR byproduct was detected in the presence of CLZ in these samples (Fig. 2, *Left 1*, *3*, *4*, and *9*). In contrast, both AtAtg4a and AtAtg4b cleaved all other remaining AtAtg8s at similar levels (Fig. 2, *Left 2* and *5*–*8*).

To further confirm these results, samples of selected AtAtg8 isoforms were separated on SDS/PAGE followed by immunoblot analyses with RLUC antibodies. An increased amount of the cleaved ShR byproduct was detected in AtAtg8a, AtAtg8d, and AtAtg8i substrates processed by AtAtg4a compared with AtAtg4b (Fig. 2, *Right I*, *II*, and *IV*). Together, these results indicate that AtAtg4a functions predominantly to generate mature AtAtg8s. In addition, AtAtg4b-mediated differential cleavage of AtAtg8s suggests possible nonredundant roles for some AtAtg8s in vivo.

In *Arabidopsis*, AtAtg8h and AtAtg8i lack C-terminal extension and ends with the key Gly residue exposed (Fig. 1*A*), suggesting that these isoforms can be conjugated with PE without AtAtg4-mediated cleavage in vivo. However, our synthetic substrates contain the C-terminal ShR after the Gly residue. Therefore, we investigated if AtAtg4 proteases can cleave AtAtg8h and AtAtg8i. In our NASCA and immunoblot assays, both AtAtg4a and AtAtg4b processed AtAtg8h efficiently (Fig. 2, *Left 8* and *Right III*). Interestingly, AtAtg4a processed AtAtg8i more efficiently compared with AtAtg4b (Fig. 2, *Left 9* and *Right*

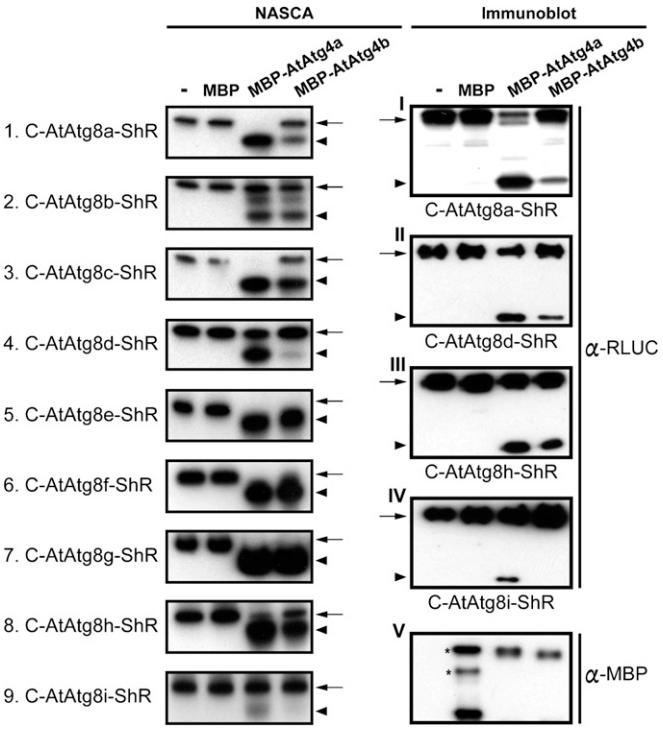

Fig. 2. Differential cleavage of AtAtg8s by AtAtg4a and AtAtg4b in vitro. Cleavage efficiency of nine AtAtg8 substrates evaluated by NASCA assay in the presence of coelenterazine, CLZ (*Left*). Confirmation of selected NASCA results by immunoblot analyses using antibodies against ShR (α-RLUC) (*Right*, *I*–*IV*). Immunoblot analysis using antibodies against MBP (α-MBP) shows similar amount of AtAtg4a and AtAtg4b inputs used in the assay (*Right*, *V*). Lanes from *Left* to *Right*: lane 1, synthetic substrates; lane 2, synthetic substrates with MBP; lane 3, synthetic substrates with MBP-AtAtg4a; lane 4, synthetic substrates with MBP-AtAtg4b. Arrows and arrowheads represent the uncleaved substrate and the cleaved ShR byproduct, respectively. MBP, maltose-binding protein. Asterisks in *Right*, *V* indicate bands with nonspecific interactions with α-MBP antibody. All experiments have been performed at least two times.

IV). These results indicate that AtAtg4s exhibit preferential substrate specificity toward AtAtg8h and AtAtg8i even though they contain the terminal Gly residue and are not initially processed in vivo. Transport of AtAtg8i to the vacuole in vivo requires AtAtg4 activity because deconjugation from the lipidated AtAtg8i (AtAtg8i-PE) requires AtAtg4 activity (13). Therefore, the differential processing activity of AtAtg4s observed here may suggest a differential rate for the PE deconjugation step that is required for recycling of AtAtg8h and AtAtg8i in vivo.

The Conserved C-Terminal Gly Residue of AtAtg8s Is Required for Processing by AtAtg4s. The C-terminal Gly residue in Atg8s is important for cleavage by Atg4s in yeast and mammalian systems (6, 16). To examine the importance of the Gly residue in AtAtg8s, we substituted the Gly with an alanine (GtoA). Purified mutant C-AtAtg8a(GtoA)-ShR synthetic substrate was tested for processing by AtAtg4. The ShR byproduct from the AtAtg8a mutant was not detected in the presence of either AtAtg4a or AtAtg4b (Fig. 3*A*, *Upper* lanes 3 and 5) compared with the wild-type AtAtg8a substrate (Fig. 3*A*, *Upper* lanes 2 and 4). In immunoblot analyses, the ShR product was detected only in the wild-type AtAtg8a but not with the mutant AtAtg8a(GtoA) substrate (Fig. 3*A*, *Lower* lanes 3 and 5). These results indicate that similarly to yeast and mammalian systems, the Gly residue at the C terminus of AtAtg8a is important for cleavage by AtAtg4 proteases.

As noted above, AtAtg8i lacks C-terminal extension and ends with the Gly exposed (Fig. 1*A*). Therefore, we tested if the Gly in AtAtg8i is also important for processing by AtAtg4s. The amount of purified mutant AtAtg8i(GtoA) cleaved by AtAtg4s was below the detection limit in NASCA assay (Fig. 3*B*, *Upper*) and immunoblot analyses (Fig. 3*B*, *Lower*). These results demonstrate that the C-terminal Gly residue is important for cleavage by AtAtg4s.

***Arabidopsis* AtAtg4a and AtAtg4b Do Not Process a Human Atg8 Homolog, Microtubule-Associated Protein 1 Light Chain 3a.** Because autophagy is a highly conserved biological process among different organisms, we tested if AtAtg4 cysteine proteases can cleave a human Atg8 homolog, LC3a. For this, we purified C-hLC3a-ShR from the bacterial expression system and cleavage assay was performed with AtAtg4a and AtAtg4b. Neither AtAtg4a nor AtAtg4b was able to process hLC3a (Fig. 3*C*, lanes 3 and 4). These results indicate that AtAtg4s have specificity toward AtAtg8s. Furthermore, these results show that although the Atg8 processing mechanism is conserved among different organisms, Atg4 proteases are not interchangeable between the organisms.

AtAtg4a Is Catalytically More Active than AtAtg4b. Because AtAtg4a and AtAtg4b exhibited differential AtAtg8 substrate cleavage efficiency (Fig. 2), we set out to determine kinetic differences between the two AtAtg4s against the AtAtg8e substrate. For this assay we incubated an equal amount of either AtAtg4a or AtAtg4b with different amounts of the AtAtg8e and determined the amount of the cleaved ShR byproduct (Fig. 3*D*). Saturation was reached for AtAtg4a at ~3 μM of the AtAtg8e substrate compared with 5.7 μM for AtAtg4b. Using the cleaved ShR product concentration, we determined Michaelis–Menten kinetics (V_{max} and K_m) for AtAtg4a and AtAtg4b (Fig. 3*D*). K_m values of AtAtg4a and AtAtg4b are 1.9 μM and 1.6 μM, respectively. V_{max} of AtAtg4a (V_{max} = 4.3) is two times higher than that of AtAtg4b (V_{max} = 2.2). These results indicate that although both AtAtg4a and AtAtg4b have similar substrate affinities, the AtAtg4a has higher catalytic activity.

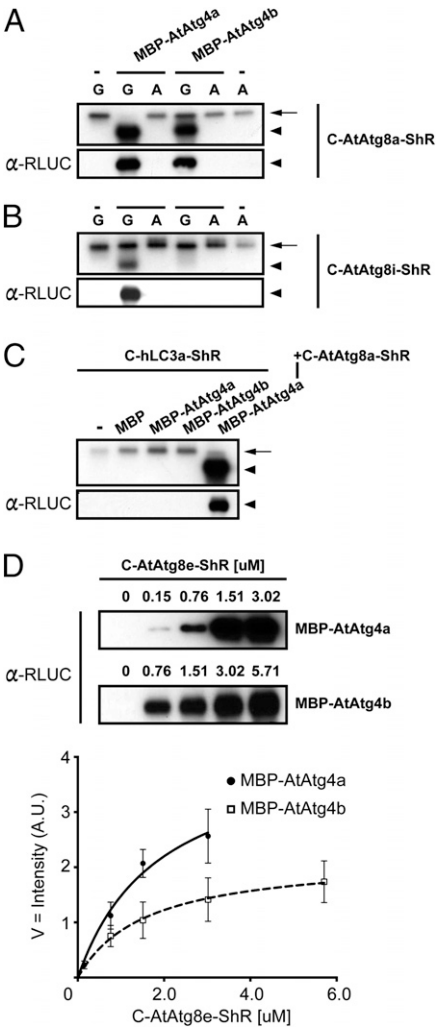

Fig. 3. Kinetics of AtAtg4a and AtAtg4b cysteine proteases. (*A* and *B*) The conserved glycine residue in AtAtg8 is required for the AtAtg4-mediated processing. Substitution of the glycine (G) with an alanine (A) completely abolished cleavage of C-AtAtg8a-ShR (*A*) and C-AtAtg8i-ShR (*B*) substrates. NASCA assay results (*Upper*) and the immunoblot analyses with α-RLUC antibodies (*Lower*) are shown. Single dash lines on the top indicate no addition of MBP-AtAtg4s. Arrows and arrowheads represent the uncleaved substrate and the cleaved ShR byproduct respectively. (*C*) The human LC3a substrate (C-hLC3a-ShR) is not processed by AtAtg4s. *Upper* is a cleavage assay by NASCA, and *Lower* is the immunoblot analysis with α-RLUC antibodies. C-AtAtg8a-ShR is used as a positive control. Single dash line on top represents no addition of AtAtg4. Arrows and arrowheads represent the uncleaved substrate and the cleaved ShR byproduct, respectively. (*D*) Michaelis–Menten kinetics of AtAtg4a and AtAtg4b activities derived from the immunoblot intensities of C-AtAtg8e-ShR obtained after cleavage assays. Values, average ± SEM (n = 3). Numbers on the top of each immunoblot are concentrations of the C-AtAtg8e-ShR substrate. In the immunoblot of AtAtg4b, 0.15 μM of the C-AtAtg8e-ShR input was under the detection limit. A.U. indicates arbitrary unit of immunoblot intensity after normalization as described in *SI Materials and Methods*.

Hydrogen Peroxide Reversibly Inhibits AtAtg4 Cysteine Protease Activity. Human Atg4s (hAtg4s) have been shown to be sensitive to reactive oxygen species (ROS), specifically H_2O_2, that are produced during nutrient starvation (17). Therefore, we tested if AtAtg4s activity is regulated by H_2O_2. Purified AtAtg4a or AtAtg4b was preincubated with a different concentration of H_2O_2 for 5 min and then the AtAtg8f substrate was added. Cleavage of AtAtg8f by AtAtg4s was significantly reduced as H_2O_2 concentration was increased (Fig. 4*A*). This inhibition was

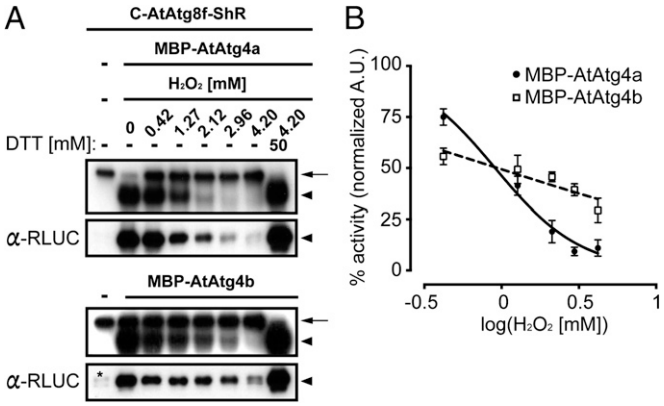

Fig. 4. Reversible inhibition of AtAtg4s activity by hydrogen peroxide. (*A*) Dose-dependent inhibition of hydrogen peroxide (H_2O_2) for AtAtg4s to process C-AtAtg8f-ShR substrate. Addition of reducing agent DTT restored AtAtg4 activity. Numbers and dash lines on the top represent amount of H_2O_2 added to each reaction and no addition of indicated components, respectively. *Upper* and *Lower* boxes are the NASCA result in the presence of CLZ and the corresponding immunoblot result with α-RLUC antibodies, respectively. Asterisk in the immunoblot of the MBP-AtAtg4b cleavage assay is nonspecific degradation. Arrows and arrowheads represent the uncleaved substrate and the cleaved ShR byproduct, respectively. (*B*). Different inhibitory behavior of MBP-AtAtg4a and MBP-AtAtg4b activity to H_2O_2 treatment. Normalized individual band intensities from immunoblots shown in *A* fitted to a curve. Under low H_2O_2 concentration, residual normalized MBP-AtAtg4a activity was higher than MBP-AtAtg4b. Under high H_2O_2 concentration, an opposite result was observed. *X* axis is a log scale of H_2O_2 concentration. Values, average ± SEM ($n = 3$).

reversible by treatment with DTT (Fig. 4*A*), indicating that H_2O_2 reversibly inhibits AtAtg4 activity in vitro.

We next determined the half maximal inhibitory concentration (IC_{50}) based on the dose-dependent inhibition of AtAtg4 activity. IC_{50} of AtAtg4a and AtAtg4b was estimated to be 0.91 and 0.94 mM of H_2O_2, respectively (Fig. 4*B*). However, the dose-dependent inhibition of AtAtg4a showed different kinetic behavior compared with AtAtg4b. The AtAtg4a inhibition was fitted to the inverse sigmoid curve compared with AtAtg4b that showed a linear regression. In addition, activity of AtAtg4b after normalization was higher than AtAtg4a at a high concentration of H_2O_2 (Fig. 4*B*). As H_2O_2 concentration increased from 0.42 to 4.2 mM, AtAtg4b was more resistant to oxidative stress because only 25% of AtAtg4b activity was eliminated compared with 65% of AtAtg4a activity (Fig. 4*B*). These results suggest different sensitivity of AtAtg4a and AtAtg4b for H_2O_2. Furthermore, comparison of residual activity of AtAtg4b with that of AtAtg4a under high H_2O_2 concentration indicates that AtAtg4b is more resistant than AtAtg4a in vitro.

AtAtg8a Synthetic Substrate Is Efficiently Processed in Vivo and Requires AtAtg4 Proteases. To test if endogenous AtAtg4 can cleave the synthetic substrates in plants, we generated wild-type Col-0 and *atg4a4b* double-mutant (13) plants expressing the C-AtAtg8a-ShR. Confocal microscopy analyses of transgenic plants confirmed the expression of C-AtAtg8a-ShR in the cytoplasm (Fig. S2). The transgenic seedlings were subjected to nitrogen starvation to induce autophagy (*SI Materials and Methods*). About 12 h before confocal microscopy analyses, the seedlings were treated with 1 μM of concanamycin A that is known to inhibit degradation of autophagic bodies in the vacuole (13). In Col-0::C-AtAtg8a-ShR tissues, we observed highly abundant punctate autophagic bodies in the vacuole (Fig. 5*A*, *Upper*). To further confirm that these are autophagic bodies, we performed colocalization analysis with monodansylcadaverine (MDC), a widely used autofluorescence compound that specifically labels autophagic bodies (18) (see *SI Materials and Methods* for details). Under autophagy inducing conditions, many Citrine fluorescent vesicles colocalized with MDC-labeled autophagic bodies, both in the vacuole (Fig. S3 *A* and *B*, yellow and white arrowheads) and in the cytoplasm (Fig. S3*A*, cyan arrows). These results indicate that C-AtAtg8a-ShR mimics endogenous AtAtg8a and is efficiently processed by AtAtg4s for their maturation and integration into autophagic bodies. In contrast, punctate autophagic bodies were absent in *atg4a4b*::C-AtAtg8a-ShR transgenic plant tissues (Fig. 5*A*, *Lower*). In Col-0::C-AtAtg8a-ShR plants, we observed diverse sizes of speckles that were localized with the *trans* vacuolar strands in the cytoplasm (Fig. 5*A*, arrowheads). We reasoned that these speckles might be autophagosomes that were not getting delivered to the vacuole.

To further confirm that the AtAtg8a substrate is processed in vivo, we performed immunoblot analysis of total protein extracted from Col-0::C-AtAtg8a-ShR and *atg4a4b*::C-AtAtg8a-ShR plant leaves after nitrogen starvation. In Col-0::C-AtAtg8a-ShR plants, a high amount of ShR byproduct was observed (Fig. 5*B*, lanes 2–4). In contrast, ShR byproduct was absent in *atg4a4b*::C-AtAtg8a-ShR plants (Fig. 5*B*, lane 5). Together these results show that our AtAtg8a synthetic substrate is efficiently processed by endogenous AtAtg4s.

Efficient Monitoring of in Vivo AtAtg4 Activity by BRET. As discussed above, our synthetic substrates could also be used to monitor cleavage of AtAtg8s by AtAtg4s using BRET. To determine if we can use BRET to measure in vivo AtAtg4 cleavage efficiency, we induced autophagy by subjecting Col-0::C-AtAtg8a-ShR and *atg4a4b*::C-AtAtg8a-ShR transgenic plants to nitrogen starvation. The observed 10 times higher blue luminescence in transgenic plants expressing C-AtAtg8a-ShR indicates stable expression of the substrate compared with wild-type Col-0 background (Fig. 5*C*). In the converted BRET ratio (yellow fluorescence/blue luminescence), a statistically significant increase in BRET ratio was observed in *atg4a4b*::C-AtAtg8a-ShR plants compared with Col-0::C-AtAtg8a-ShR (Fig. 5*D*, $P < 0.005$). In *atg4a4b*::C-AtAtg8a-ShR plants, the substrate is not processed and hence intramolecular BRET occurs more efficiently in the presence of CLZ. In contrast, AtAtg4s cleave the AtAtg8a substrate, resulting in reduced BRET ratio in Col-0::C-AtAtg8a-ShR transgenic plants. Taken together, these results show that the endogenous AtAtg4 cysteine proteases can effectively cleave our synthetic substrate in vivo. Furthermore, AtAtg4 cleavage of the AtAtg8a substrates representing de novo formation of autophagosomes can be monitored by BRET-based assays.

Discussion

Atg4-mediated conjugation and deconjugation of Atg8s are essential for autophagosome biogenesis (1). *Arabidopsis* contains nine AtAtg8 and two AtAtg4 family members with high amino acid sequence similarity (9, 10). The reason for AtAtg8 and AtAtg4 diversification in plants remains to be addressed. Because AtAtg8 family members are differentially expressed in different organs, tissues, and cell types under different stress conditions (11, 12), it has been hypothesized that individual AtAtg8 members may function under specific developmental and/or stress conditions to target specific cargo(es) for degradation or recycling. However, functional redundancy has hampered the analysis of individual AtAtg8s and substrate specificity of AtAtg4s in *Arabidopsis*. To elucidate substrate specificity of different AtAtg4s with different AtAtg8s, we designed unique C-AtAtg8-ShR synthetic substrates. Our systematic analyses using purified AtAtg8 substrates and AtAtg4s indicate that AtAtg4a is more efficient in cleaving all AtAtg8s in vitro compared with the less active AtAtg4b. We found that this is not due to differential affinity of AtAtg4s to the substrate because both

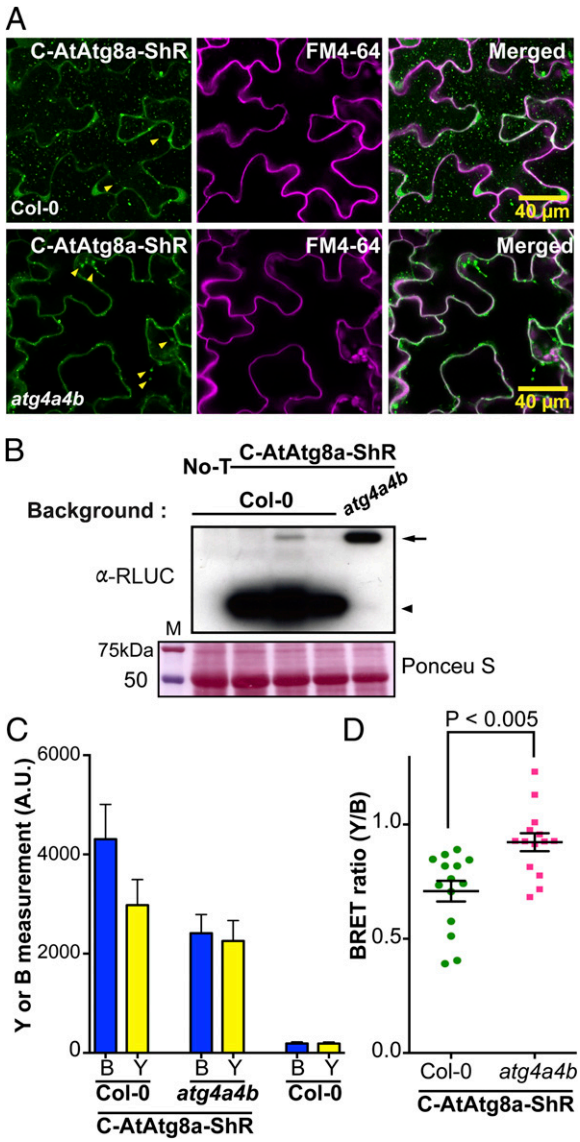

Fig. 5. Efficient processing of AtAtg8 synthetic substrate in transgenic *Arabidopsis* plants. (*A*) Subcellular localizations of the C-AtAtg8a-ShR substrate in transgenic Col-0 wild-type (*Upper*) or *atg4a4b* mutant (*Lower*) plants under nitrogen limitation condition. Citrine fluorescence was observed in the cytoplasm and in the vacuole as punctate structures representing C-AtAtg8a in the leaf epidermal cells of Col-0::C-AtAtg8a-ShR transgenic plant leaves (*Upper*). In the *atg4a4b*::C-AtAtg8a-ShR transgenic plants, Citrine fluorescence was observed in the cytoplasm including *trans* vacuolar strands but not in the vacuole (*Lower*). FM4-64 dye was used to visualize the plasma membrane (*Center*). Arrowheads indicate the diverse sizes of speckles in the *trans* vacuolar strands. (Scale bar = 40 μm.) (*B*) Immunoblot analyses to confirm cleavage of the C-AtAtg8a-ShR by AtAtg4s in transgenic *Arabidopsis*. Protein extracted from nitrogen-deprived seedlings was separated on SDS/PAGE and immunoblot was probed with α-RLUC (*Upper*). Reduced full-length C-AtAtg8a-ShR and increased ShR byproduct were detected in Col-0::C-AtAtg8a-ShR transgenic plants (*Upper*, lanes 2–4). Full-length C-AtAtg8a-ShR was highly accumulated in *atg4a4b*::C-AtAtg8a-ShR transgenic plants (*Upper*, lane 5). Nontransgenic wild type Col-0 (No-T) was used as a control (*Upper*, lane 1). Ponceau S stained blot shows loading amount of total protein extract (*Lower*). M, molecular size marker. Arrow and arrowhead represent the uncleaved substrate and the cleaved ShR byproduct, respectively. (*C*) Measurement of blue luminescence (B) and yellow fluorescence (Y) in transgenic *Arabidopsis* Col-0 and *atg4a4b* shows expression of C-AtAtg8a-ShR. Measurement in Col-0 nontransgenic plant shows background levels of B and Y. (*D*) Plotting of individual BRET ratios converted from individual seedlings shows statistically significant increased BRET ratios ($P < 0.005$) resulting from high accumulation of the uncleaved C-AtAtg8a-ShR in the *atg4a4b* mutant compared with Col-0 transgenic *Arabidopsis*. Y and B are intensity of yellow fluorescence and blue luminescence, respectively. Values, average ± SEM ($n = 3$).

AtAtg4s showed similar affinity to the C-AtAtg8e-ShR. Kinetic analyses also indicated that the processing activity of AtAtg4a is two times higher than that of AtAtg4b. These findings indicate that AtAtg4a has a broad substrate range and functions as a predominant cysteine protease to activate autophagy in *Arabidopsis*. Similarly in humans, where there are four Atg4 homologs (hAtg4a–4d), hAtg4b has been shown to be more active in cleaving four hAtg8-GST (GATE-16, LC3b, Atg8L, and GABARAP) synthetic substrates in vitro compared with hAtg4a (16). Unlike *Arabidopsis* AtAtg4s, lower cleavage efficiency of hAtg4a is due to lower substrate affinity compared with hAtg4b (16). These studies suggest that unlike yeast that contains single Atg4 and Atg8, a combination of specific Atg4-Atg8 pairs in plants and humans could function to activate autophagy during specific biological processes.

Generally, cysteine residues in polypeptides are one of the major targets for posttranslational modification under oxidative stress conditions (19). We observed dose-dependent inhibition of AtAtg4 cysteine protease activity under oxidative stress in vitro. Interestingly, AtAtg4 activity is restored in the presence of DTT, indicating that the oxidation-induced inhibition of AtAtg4 activity is reversible. Both AtAtg4a and AtAtg4b have similar IC_{50} for inhibition by H_2O_2 but they exhibited different inhibitory behavior at different H_2O_2 concentrations. Human Atg4 activity has also been shown to be sensitive to H_2O_2 in vitro and is under redox regulation (17). In human cells, starvation-induced H_2O_2 can activate autophagy (17). ROS can also induce autophagy in *Arabidopsis* (20). It is proposed that nutrient starvation of human cells induces an increase in the local H_2O_2 concentration at the mitochondria, inactivating hAtg4s to suppress deconjugation activity, and in turn facilitating conjugation of hAtg8 to PE and autophagosome formation (17). Once the autophagosome matures and fuses to the lysosome, hAtg4 at the lysosome becomes active because of a lower level of H_2O_2 at this location leading to delipidation and recycling of hAtg8 (17). Because AtAtg4a is more sensitive to H_2O_2 than AtAtg4b under high H_2O_2 concentration, we hypothesize that under prolonged exposure to oxidative stress conditions, plants might use AtAtg4b to activate autophagy. Our AtAtg8 substrates described here in combination with *Arabidopsis atg4* mutants should facilitate further dissection of the precise role of different AtAtg4s during the oxidative stress response in *Arabidopsis*.

Most studies described to date in plants have relied on roots or protoplasts to monitor autophagy in vivo (2, 13). This is not ideal for investigation of the role of autophagy in biological processes that occurs in mature plant leaf such as photosynthesis and responses to different pathogens (2, 11). Using transgenic *Arabidopsis* expressing our C-AtAtg8a-ShR synthetic substrate, we were able to observe autophagosomes in leaf tissue sharing similar characteristics to those observed in *Arabidopsis* roots or seedlings expressing GFP-AtAtg8a (13). Our results also indicated that the ShR fusion at the C terminus of the AtAtg8a has no effect on AtAtg8a localization and biogenesis of autophagosomes. Our results further confirmed that processing by AtAtg4s is required for autophagosome formation because *atg4a4b* double mutant plants fail to accumulate C-AtAtg8a-tagged autophagic bodies in the vacuole even in the presence of concanamycin A (Fig. 5*A*). Therefore, our transgenic *Arabidopsis* expressing the AtAtg8 substrate will be a valuable tool to monitor autophagy in plant leaves under different biological processes.

Although punctate autophagosome structures observed in the vacuole of wild-type plants were absent in *atg4a4b* plants, we did observe a few punctate-like structures in the cytoplasm and

PLANT BIOLOGY

in the *trans* vacuolar strand of the *atg4a4b* mutant expressing C-AtAtg8a-ShR. These punctae-like structures might be aggregate forms of C-AtAtg8a-ShR because similar subcellular compartments were observed in *atg4a4b* expressing GFP-AtAtg8a (13). Furthermore, solubility of GFP-AtAtg8a from *atg4a4b* mutant was decreased in a nonionic Triton X-100 detergent but increased in deoxycholate ionic detergent. Therefore, the authors suggested that big punctae-like structures might be aggregate forms of GFP-AtAtg8a (13). Some of the mature C-AtAtg8a in Col-0 that we observed as punctae-like structures in the cytoplasm (Fig. 5*A*) could be aggregates. Alternatively, these punctae-like structures might be autophagosomes but are not delivered to the vacuole. Consistent with this, we observed increased accumulation of unprocessed C-AtAtg8a-ShR in *atg4a4b* mutant (Fig. 5*B*, lane 5) compared with Col-0 (Fig. 5*B*, lanes 2–4) in which endogenous AtAtg4s could efficiently process AtAtg8a substrate resulting in decreased C-AtAtg8a-ShR and increased cleaved ShR byproduct. We did observe some variability in the amount of C-AtAtg8a-ShR in Col-0::C-AtAtg8a-ShR plants (Fig. 5*B*, lanes 2–4). This could be due to variability in nutrient stress received by individual plants corresponding to a differential rate of autophagy.

Importantly, the in vivo BRET ratio in Col-0 was significantly lower compared with *atg4a4b* mutant, indicating efficient processing of the substrate in Col-0 but not in *atg4a4b* mutant. We did observe a very low BRET ratio of <0.4 in few Col-0::C-AtAtg8a-ShR plants. Because ~0.4 BRET ratio ($\lambda_{530}/\lambda_{470}$) is normally observed in the *Renilla* luciferase emission spectrum (14), we excluded the extremely low BRET ratios from our analysis and this did not affect our conclusions. Taken together, AtAtg4s can efficiently cleave our BRET-based AtAtg8a sensor in transgenic plants and the synthetic substrate mimics endogenous AtAtg8a in autophagosome biogenesis.

Our unique AtAtg8 synthetic substrate and NASCA assay described here provide a very robust, sensitive measurement of AtAtg4 activity in vitro. The released ShR byproduct from the full-length AtAtg8 substrate is easy to detect AtAtg4 activity compared with a widely used SDS/PAGE and immunoblotting method (21). Our data also demonstrate that the synthetic substrate is efficiently used to monitor autophagosome biogenesis in vivo. Therefore, the BRET-based assay could be used to monitor the rate of autophagy in leaf tissue during a specific biological process. Recently, fluorescence resonance energy transfer (FRET)-based human Atg8 substrates have been described for quantitative measurement of hAtg4 activity in vitro and in mammalian cell lysates (22). Although the FRET-based assay is highly sensitive, the direct excitation of the acceptor fluorophore by the external light for activation of the donor fluorophore influences successful FRET (23). Because the luciferase enzyme in BRET is the donor, it can emit photons without fluorescence excitation (23). In our BRET-based AtAtg8 substrates, the resonance energy to activate the Citrine acceptor fluorescence protein is generated by decarboxylation of CLZ. BRET-based high throughput assays require less expensive instrumentation and setup. In living plant tissues, FRET signal has to be significantly higher to discriminate from high background autofluorescence caused by chlorophyll and thick cell walls. Therefore, our BRET-based substrates will not only facilitate investigation of AtAtg4 activity in vitro but also monitor de novo biogenesis of autophagosomes in living plant tissues.

Autophagy is a tightly regulated process and failure to activate or shut off autophagy in a timely fashion will have a deleterious effect on the organism. The identification of autophagy regulators will not only advance our mechanistic understanding of autophagy but will also facilitate modulation of autophagy for practical applications. Although some chemical modulators of mammalian autophagy have been identified (24), these modulators are ineffective in plants. Therefore, the BRET-based AtAtg8 substrates described here will allow us to screen for autophagy regulators under in vitro and in vivo conditions in a high throughput manner.

Materials and Methods

Details of plasmid construction, expression and purification of recombinant proteins of AtAtg8s and AtAtg4s are described in *SI Materials and Methods*. NASCA and immunoblot assays used for the analyses of AtAtg4-mediated cleavage of AtAtg8 are detailed in *SI Materials and Methods*. Generation of transgenic plants, in vivo BRET analyses under nitrogen starvation, and confocal microscopy are described in *SI Materials and Methods*.

ACKNOWLEDGMENTS. We thank Drs. Albrecht von Arnim, Andrew Hayward, and Meenu Padmanabhan for insightful discussion and for critical reading of the manuscript, Dr. Kohki Yoshimoto for *atg4a4b* seeds, and Dr. Gitta Coaker for access to the luminometer. This work is supported by University of California, Davis and by National Science Foundation Molecular and Cellular Biosciences-1355459 funds (to S.P.D.-K.).

1. He C, Klionsky DJ (2009) Regulation mechanisms and signaling pathways of autophagy. *Annu Rev Genet* 43:67–93.
2. Hayward AP, Dinesh-Kumar SP (2011) What can plant autophagy do for an innate immune response? *Annu Rev Phytopathol* 49:557–576.
3. Li F, Vierstra RD (2012) Autophagy: A multifaceted intracellular system for bulk and selective recycling. *Trends Plant Sci* 17(9):526–537.
4. Liu Y, Bassham DC (2012) Autophagy: Pathways for self-eating in plant cells. *Annu Rev Plant Biol* 63:215–237.
5. Ohsumi Y (2001) Molecular dissection of autophagy: Two ubiquitin-like systems. *Nat Rev Mol Cell Biol* 2(3):211–216.
6. Kirisako T, et al. (2000) The reversible modification regulates the membrane-binding state of Apg8/Aut7 essential for autophagy and the cytoplasm to vacuole targeting pathway. *J Cell Biol* 151(2):263–276.
7. Nair U, et al. (2012) A role for Atg8-PE deconjugation in autophagosome biogenesis. *Autophagy* 8(5):780–793.
8. Nakatogawa H, Ishii J, Asai E, Ohsumi Y (2012) Atg4 recycles inappropriately lipidated Atg8 to promote autophagosome biogenesis. *Autophagy* 8(2):177–186.
9. Hanaoka H, et al. (2002) Leaf senescence and starvation-induced chlorosis are accelerated by the disruption of an Arabidopsis autophagy gene. *Plant Physiol* 129(3):1181–1193.
10. Doelling JH, Walker JM, Friedman EM, Thompson AR, Vierstra RD (2002) The APG8/12-activating enzyme APG7 is required for proper nutrient recycling and senescence in Arabidopsis thaliana. *J Biol Chem* 277(36):33105–33114.
11. Hayward AP, Tsao J, Dinesh-Kumar SP (2009) Autophagy and plant innate immunity: Defense through degradation. *Semin Cell Dev Biol* 20(9):1041–1047.
12. Sláviková S, et al. (2005) The autophagy-associated Atg8 gene family operates both under favourable growth conditions and under starvation stresses in Arabidopsis plants. *J Exp Bot* 56(421):2839–2849.
13. Yoshimoto K, et al. (2004) Processing of ATG8s, ubiquitin-like proteins, and their deconjugation by ATG4s are essential for plant autophagy. *Plant Cell* 16(11):2967–2983.
14. Woo J, von Arnim AG (2008) Mutational optimization of the coelenterazine-dependent luciferase from Renilla. *Plant Methods* 4:23.
15. Subramanian C, et al. (2006) A suite of tools and application notes for in vivo protein interaction assays using bioluminescence resonance energy transfer (BRET). *Plant J* 48(1):138–152.
16. Li M, et al. (2011) Kinetics comparisons of mammalian Atg4 homologues indicate selective preferences toward diverse Atg8 substrates. *J Biol Chem* 286(9):7327–7338.
17. Scherz-Shouval R, et al. (2007) Reactive oxygen species are essential for autophagy and specifically regulate the activity of Atg4. *EMBO J* 26(7):1749–1760.
18. Biederbick A, Kern HF, Elsässer HP (1995) Monodansylcadaverine (MDC) is a specific in vivo marker for autophagic vacuoles. *Eur J Cell Biol* 66(1):3–14.
19. Pace NJ, Weerapana E (2013) Diverse functional roles of reactive cysteines. *ACS Chem Biol* 8(2):283–296.
20. Xiong Y, Contento AL, Nguyen PQ, Bassham DC (2007) Degradation of oxidized proteins by autophagy during oxidative stress in Arabidopsis. *Plant Physiol* 143(1):291–299.
21. Nakatogawa H, Ohsumi Y (2012) SDS-PAGE techniques to study ubiquitin-like conjugation systems in yeast autophagy. *Methods Mol Biol* 832:519–529.
22. Li M, Chen X, Ye QZ, Vogt A, Yin XM (2012) A high-throughput FRET-based assay for determination of Atg4 activity. *Autophagy* 8(3):401–412.
23. Xie Q, Soutto M, Xu X, Zhang Y, Johnson CH (2011) Bioluminescence resonance energy transfer (BRET) imaging in plant seedlings and mammalian cells. *Methods Mol Biol* 680:3–28.
24. Cho YS, Kwon HJ (2010) Control of autophagy with small molecules. *Arch Pharm Res* 33(12):1881–1889.